https://doi.org/10.1007/s41230-023-2168-5

Effects of mechanical vibration on filling and solidification behavior, microstructure and performance of Al/Mg bimetal by lost foam compound casting

Guang-yu Li, Feng Guan, *Wen-ming Jiang, Yuan-cai Xu, Zheng Zhang, and Zi-tian Fan

State Key Laboratory of Materials Processing and Die & Mould Technology, School of Materials Science and Engineering, Huazhong University of Science and Technology, Wuhan 430074, China

Abstract: Al/Mg bimetal was prepared by lost foam solid-liquid compound casting, and the effects of mechanical vibration on the filling and solidification behavior, microstructure and performance of the bimetal were investigated. Results show that the mechanical vibration has a remarkable influence on the filling and solidification processes. It is found that after mechanical vibration, the filling rate increases and the filling rate at different times is more uniform than that without vibration. In addition, the mechanical vibration also increases the wettability between liquid AZ91D and A356 inlays. The mechanical vibration reduces the horizontal and vertical temperature gradient of the casting and makes the temperature distribution of the whole casting more uniform. Compared to the Al/Mg bimetal without vibration, the shear strength is improved by 39.76% after the mechanical vibration is applied, due to the decrease of the inclusions and $Al_{12}Mg_{17}$ dendrites, and the refinement and uniform distribution of the Mg_2Si particles in the interface of the Al/Mg bimetal.

Keywords: lost foam casting; filling and solidification processes; Al/Mg bimetal; mechanical vibration; microstructure; mechanical properties

CLC numbers: TG146.21 **Document code:** A **Article ID:** 1672-6421(2023)06-469-11

1 Introduction

Aluminum alloy (Al alloy) and magnesium alloy (Mg alloy) are important engineering light metals, and each of them has its own advantages and disadvantages [1-5]. Al/Mg bimetal combines the advantages of the Al alloy and Mg alloy and has good comprehensive performance, therefore having broad application prospects in the weapons, automobile, aviation, aerospace, electronic 3C, etc [6-8]. Its main preparation methods include welding [9, 10], rolling [11, 12], compound casting [13, 14], and so on. As a kind of the compound casting, the lost foam solid-liquid compound casting has the advantages such as no additional fixation for the inlay is needed, beneficial for metallurgical bonding, can be strengthened by following heat treatment, the foam decomposition products are conducive to preventing metal oxidation, and suitable for preparation of complex castings [15-17]. Thus, it has great application potential in the preparation of the Al/Mg bimetal.

However, there are some inherent difficulties using lost foam solid-liquid compound casting for the preparation of Al/Mg bimetal. First, the physical properties difference between the Al alloy and Mg alloy makes the bonding difficult. Second, the interface layer of the Al/Mg bimetal is mainly composed of brittle and hard Al-Mg IMCs with poor fracture toughness, which weakens the interfacial connection strength. Third, the oxide film on the surface of the Al alloy reduces its wettability with the Mg alloy, which is easy to introduce inclusion defects in the interface. Because of the problems mentioned above, the performance of the Al/Mg bimetal is poor and needs to be improved. Therefore, the strengthening of the Al/Mg bimetal is the research focus in this field.

To improve the properties of the bimetal, many strengthening methods have been proposed, including process parameter control [18, 19], removal of the oxide film [20, 21], introduction of the interlayer [22-25], alloying [13, 16, 26, 27], heat treatment [28-30], and so on. In

***Wen-ming Jiang**

Male, born in 1982, Professor. His research interests mainly focus on the magnesium, aluminum alloys and their precision casting technology, bimetallic compound casting, and 3D printing rapid casting technology.

E-mail: wmjiang@hust.edu.cn

Received: 2022-12-14; Accepted: 2022-12-30

addition, vibration is also a potential method of strengthening bimetals. Many studies have indicated that the vibration can effectively strengthen the performance of metals with the advantages of low cost, no pollution, simple technology, and easy to operate [31-33]. The vibration is conducive to melt degassing and crystallization, can promote heat exchange, increase nucleation, and thus refine and homogenize the solidification structure [34, 35]. These strengthening effects of the vibration may also be applicable to the bimetal, but there are few relevant studies, especially in the field of the compound casting. Kumar et al. [36] investigated the effect of the ultrasonic vibration on the friction stir welded 6061Al/AZ31B Mg composite. The experimental results showed that the ultrasonic vibration could effectively reduce the thickness of the IMCs layer, promote the metal's flow and mixture in the welding line, and thus effectively inhibit the formation of defects and improve the mechanical properties of the welded parts. Finally, the ultimate tensile strength increased by 22.1%. Ji et al. [37] prepared the Al/Mg bimetal by ultrasonic assisted friction stir welding and studied the influence of ultrasonic power on the quality of joint. The results suggested that the ultrasonic mechanical and acoustic cavitation effects are beneficial to the increase of effective lap width and the fragmentation of the intermetallic compounds. With the increase of the ultrasonic power, the size of Mg-Zn IMC decreases. At 1,600 W ultrasonic power, the maximum shear load of the welded joint is 7.95 kN, which is 52.6% higher than that of the traditional process. Guan et al. [38] and Wang et al. [39] studied the effects of the mechanical vibration acceleration and vibration time on the interface structure and connection strength of the solid-liquid composited Al/Mg bimetal in the lost foam casting (LFC). This study found that the mechanical vibration had the effect of thinning the thickness of the Al-Mg IMCs layer, refining and homogenizing Mg_2Si particles, thus increasing the shear strength. Under the optimal parameters, the shear strength is 47.49 MPa. Guan et al. [40] also proposed a new ultrasonic vibration-assisted method to enhance the Al/Mg bimetal prepared by LFC. It was found that the ultrasonic vibration could not only refine the Mg_2Si particles, but also refine the Al-Mg IMCs and eliminate continuous oxidation inclusions, thus obtaining better mechanical properties than the mechanical vibration, with a shear strength up to 69 MPa.

It is well known that the microstructure and properties of the castings are closely related to the filling and solidification process of liquid metal. Although there are many research works on the filling and solidification behavior in the LFC [41-43], the introduction of solid inlays and the application of vibration field will make the filling and solidification behavior more complicated in the process of the bimetallic preparation. Previous studies had explored the effect of the vibration parameters on the microstructure and properties of the bimetal, but the filling and solidification process of the solid-liquid composited Al/Mg bimetal in the LFC without or with vibration has not been reported. Therefore, in this study, the filling and solidification process as well as their correlation with the microstructure and properties with and without vibration fields were investigated, which is of great importance for understanding the formation of the interfacial microstructure and strengthening mechanism of the Al/Mg bimetal.

2 Experimental

2.1 Materials

The Al/Mg bimetal was obtained by pouring the liquid AZ91D alloy around the solid A356 alloy with the LFC technology. The compositions of the AZ91D and A356 are listed in Table 1. The material of the foam pattern was the expandable polystyrene (EPS) with a density of 12 $kg \cdot m^{-3}$.

2.2 Preparation of composite pattern

To visually study the filling behavior, the composite pattern with a clearly visible window was prepared at first, and the preparation process was as follows:

Firstly, the cuboid A356 inserts with a height of 110 mm and edge length of 10 mm were ground to 2000 mesh to wipe off the wire cut mark. After that, the A356 inserts were washed with aqueous acid (50% HNO_3+48% HF+2% water, 30 s), alkaline solutions (20 $g \cdot L^{-1}$ NaOH+5 $g \cdot L^{-1}$ ZnO, 20 s), deionized water and absolute ethyl alcohol (ultrasonic cleaning, 10 min) in sequence. The cleaned A356 inlays were put into a plastic sealing bag and sealed for storage.

Secondly, the EPS foam was cut into different sizes and assembled with A356 inlays as well as the transparent Pyrex glass, and the shape and sizes of the composite pattern are displayed in Fig. 1.

Finally, the surface of the composite pattern was coated except the Pyrex glass side. After natural air drying, the composite pattern was put into the oven at 50 °C for standby application.

Table 1: Compositions of AZ91D and A356 alloys

Alloys	Si	Ti	Fe	Mn	Zn	Mg	Al
A356	6.81	0.017	–	–	–	0.439	Bal.
AZ91D	–	–	–	0.23	0.62	Bal.	9.08

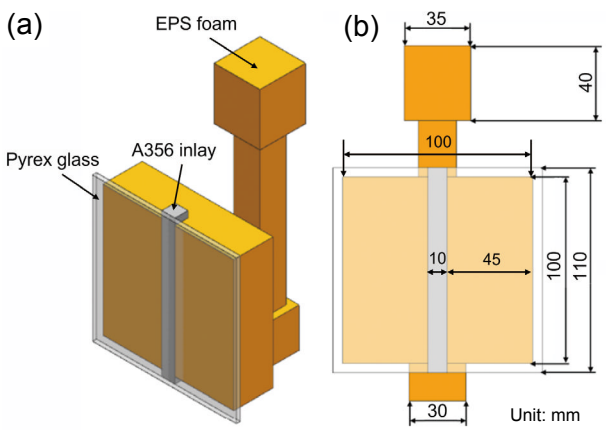

Fig. 1: Shape (a) and sizes (b) of composite pattern

2.3 Preparation of Al/Mg bimetal

The preparation principle of the Al/Mg bimetal by LFC is indicated in Fig. 2, and the specific process is as follows: Firstly, the composite pattern was put into the sand box, and the Pyrex glass on the composite pattern was attached on the observation window of the sand box with the high temperature resistant silicone rubber. Then, the 30–60 mesh's pearl sands were filled into the sand box accompanied by vibration to make the sand to fill all the spaces. After that, the vacuum pump was started to vacuum the sand box to 0.03 MPa after a plastic film was covered on the sand box's top. Finally, the AZ91D was melted under the protective atmosphere with 0.5% SF_6 and 95.5% CO_2. The molten AZ91D liquid was poured into the composite pattern at 730 °C after the mechanical vibrator. In this experiment, the mechanical vibration frequency was 35 Hz, and the amplitudes were 0.2 mm, 0.4 mm and 0.6 mm, respectively. After the melt solidified, the casting was taken out and the pouring system was removed, and finally the Al/Mg bimetal was obtained.

2.4 Test method

The Y4 high-speed camera (Integrated Design Tools Inc., China) was applied to record the whole filling process for the Al/Mg bimetal prepared by the LFC. The NI-9213 temperature collector (National Instruments, America) was employed to record the temperature variation during filling and solidification. The temperature data were collected at 16 locations as shown in Fig. 3. The microstructure of the Al/Mg bimetal was observed with a Quanta 200 scanning electron microscope (SEM) (FEI, America). The shear strengths were obtained by a push-out test (three samples for each parameter) with an AG-IC 100 kN material high temperature durability testing machine (Shimadzu, Japan), and the test philosophy has been introduced in our previous literature [44].

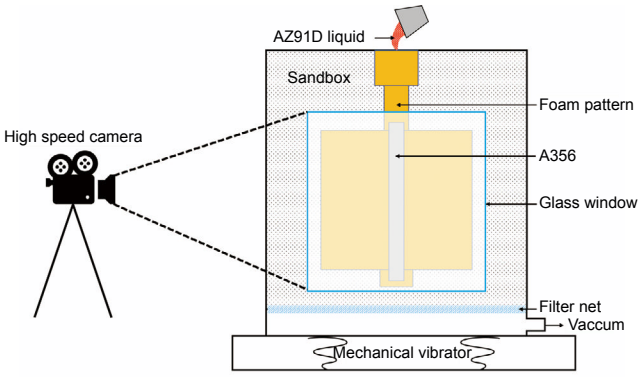

Fig. 2: Preparation principle of Al/Mg bimetal by LFC process

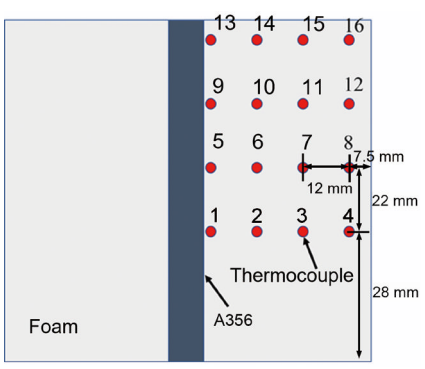

Fig. 3: Locations of temperature data collected

3 Results

3.1 Filling process

Figure 4 shows the filling process of the Al/Mg bimetal by LFC with a high-speed camera. Figures 4(a1)–(a8) and (b1)–(b8) are the results without and with vibration (0.6 mm amplitude), respectively.

It can be seen that without vibration, the filling speed of the liquid metal on both sides of the A356 inlay is obviously inconsistent from the initial stage to the middle stage (0–0.6 s), as exhibited in Figs. 4(a2)–(a4). In the second half of the filling (0.6–1.8 s), the filling speeds on both sides of the A356 inlay are similar, as displayed in Figs. 4(a5)–(a7). It can be found that the filling speed is fast at first and then slow throughout the filling process, and the liquid metal takes a total of 2.2 s to fill the cavity. Another interesting phenomenon is that the liquid metal fills the cavity in a concave shape, which is called the wall attachment effect, which is commonly seen in the filling process of the LFC under high vacuum [39, 45].

However, the introduction of the A356 inlay produces some different phenomena. The filling of the liquid metal is not concave as a whole, but is concave on both sides of the A356 inlay, and the wall attachment effect of the liquid metal on the casting wall side is greater than that on the A356 side.

Enlarge the local region of Fig. 4(a3) to further observe the interaction among the liquid metal, solid A356 inlay and foam, as shown in Fig. 5, it is found that the foam decomposes into gaseous and liquid products under the action of high-temperature liquid metal during the filling process of the LFC, and these decomposition products can be discharged through the casting wall (composed of permeable paint) finally. However, it can be seen from Fig. 5 that the existence of the aluminum inlay causes some gaseous products (black part) and liquid products (dark gray part) to gather around the aluminum inlay. This may be detrimental to a good combination between the Al and Mg alloy.

The difference of the filling velocity between the two sides of the A356 inlay is smaller under the vibration, indicating that the filling process is more stable. The filling velocity of the liquid metal still follows the principle of fast at first and then slow, but the overall filling time is reduced to 1.9 s, indicating that the filling velocity increases after the application of the vibration. The liquid metal is still filled in concave shape, but the concave depth is obviously greater than that without vibration, which indicates that the mechanical vibration increases the wall attachment effect in the filling process.

Figure 6 is a locally enlarged image of the Al/Mg bimetallic filling front before and after mechanical vibration at a filling time of 0.6 s. As can be seen from Fig. 6(a), when no vibration is applied, the flow front of the liquid metal is irregular,

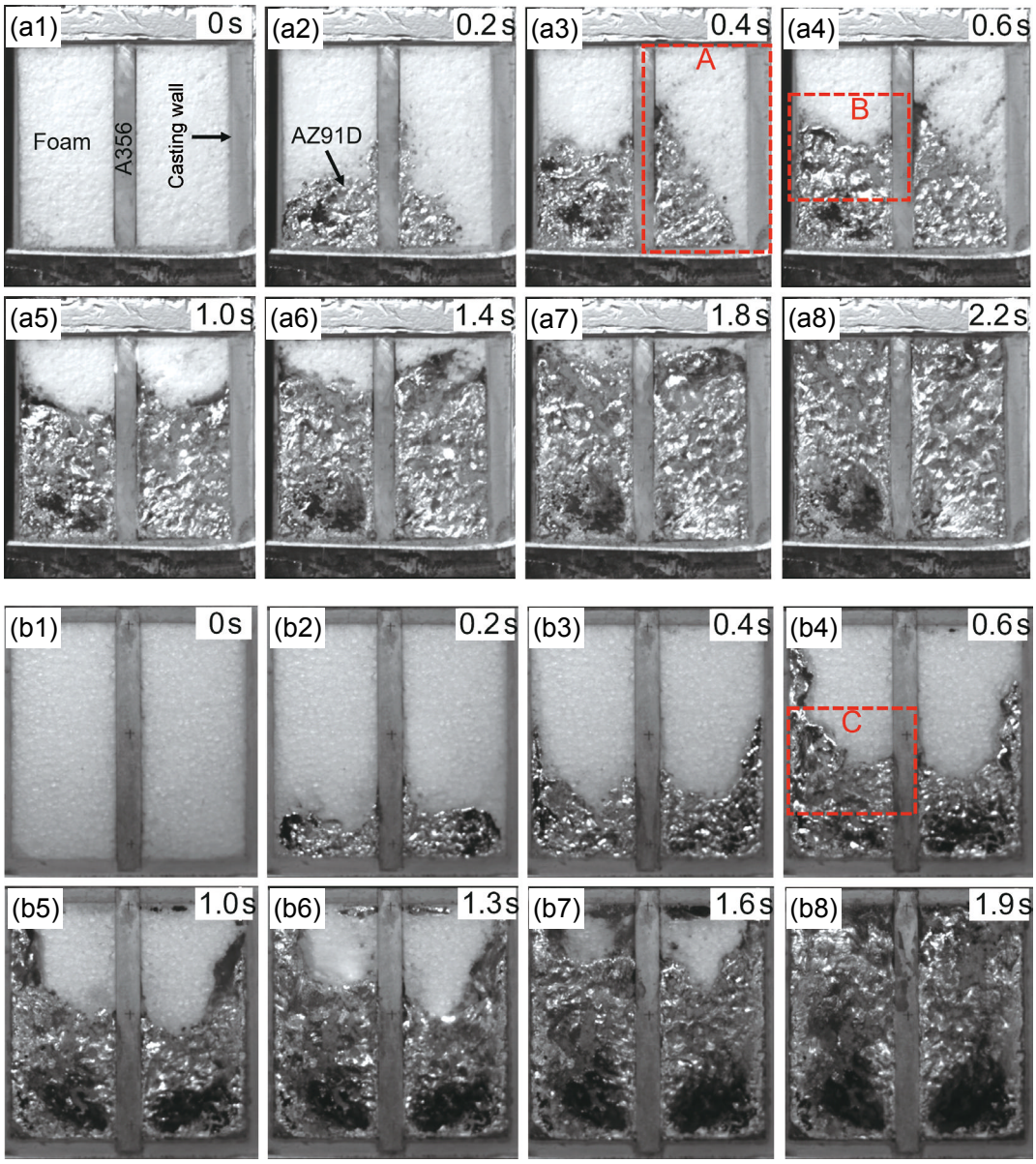

Fig. 4: Filling process of Al/Mg bimetal at different times: (a1–a8) without vibration; (b1–b8) with vibration

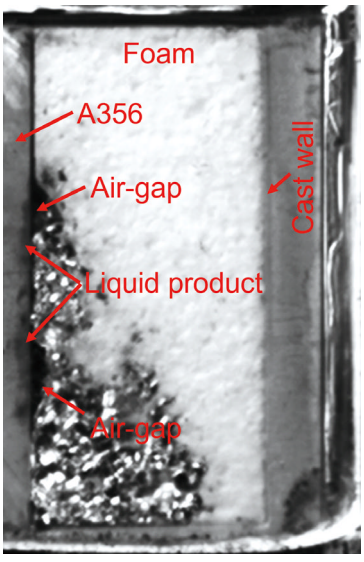

Fig. 5: Enlarged image of Area A in Fig. 4(a3)

showing a zigzag shape. After the mechanical vibration is applied, the wall attachment effect of the filling front near the casting wall is more obvious, as demonstrated in Fig. 6(b). In addition, there is a small air gap between the flow front and the A356 insert without vibration. After the mechanical vibration is applied, the air gap almost disappears and the liquid AZ91D and A356 inlay surface are in closer contact, suggesting that the vibration may increase the wettability between the metallic liquid and solid A356 inlay.

The filling time of the Al/Mg bimetal was also tested for different vibration intensities, and the results are exhibited in Fig. 7. It can be found that in the absence of the vibration, the filling time of the Al/Mg bimetal is about 2.2 s. The filling time of the Al/Mg bimetal is significantly reduced to about 1.6 s after the application of a mechanical vibration with an amplitude of 0.2 mm. As the amplitude continues to increase, the filling time increases to 1.8 s (0.4 mm amplitude) and 1.9 s (0.6 mm amplitude), respectively. This indicates that the mechanical

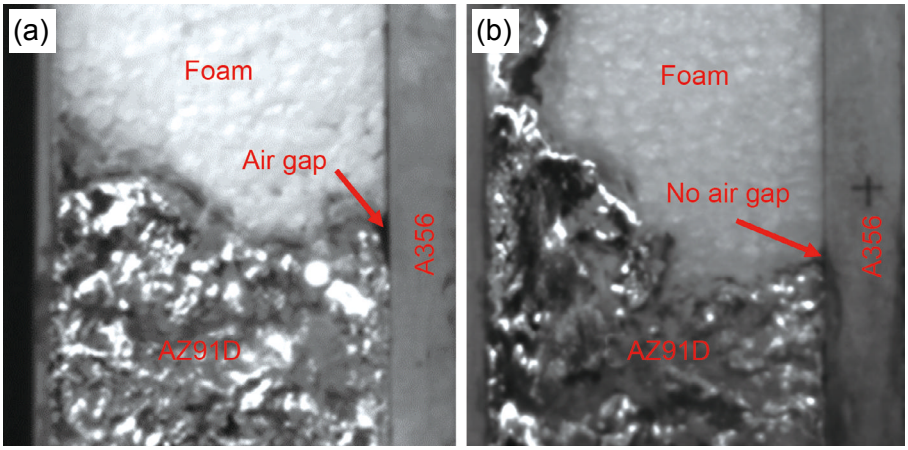

Fig. 6: Partial enlarged drawing of the filling front for AZ91D liquid at 0.6 s: (a) without vibration corresponding to Region B in Fig. 4(a4); (b) with vibration corresponding to Region C in Fig. 4(b4)

vibrations are beneficial for increasing the filling rate, but the filling rate does not increase with increasing amplitude; it shows a trend of firstly increase and then decrease.

3.2 Solidification process

To study the effect of mechanical vibrations on the solidification process of the Al/Mg bimetal, the temperature curves along the horizontal and vertical directions of the bimetal bar were selected for analysis.

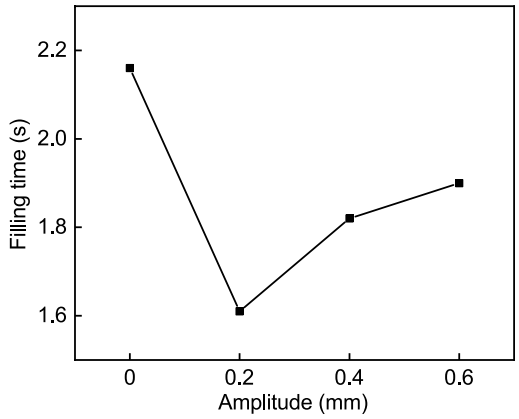

Fig. 7: Filling times of Al/Mg bimetal at different amplitudes

Figure 8 shows the temperature curves along the horizontal direction (corresponding to the temperature measurement points 9, 10, 11, and 12 in Fig. 3) before and after mechanical vibration. It can be seen that, no matter whether or not the vibration is applied, there is a great temperature difference between different temperature measuring points in the horizontal direction in the initial stage of the solidification, and with the increase of solidification time, the temperature between different locations gradually tends to be consistent. In addition, by comparing the temperature curves in Regions I and II in Fig. 8, it can be seen that, compared to the Al/Mg bimetal without vibration, the temperature curves of the different measurement points in the horizontal direction are closer after the mechanical vibration is applied. This indicates that, during the initial phase of cooling, the horizontal temperature gradient with the mechanical vibration is smaller than that without vibration, that is, the vibration can make the distribution of the horizontal temperature more uniform.

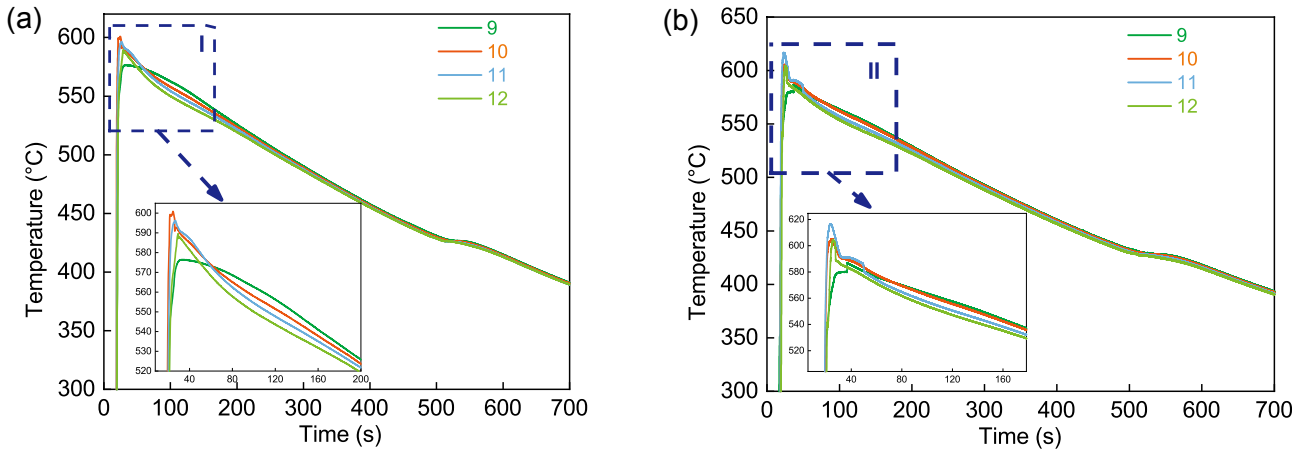

Fig. 8: Temperature curves in horizontal direction without (a) and with (b) vibration

The maximum temperatures at the different temperature curves in Fig. 8 were counted and the results are shown in Table 2. It can be found that the highest temperature in the horizontal direction near the A356 inlay and casting wall is lower than the temperature in the middle two positions, since the low temperature of the A356 inlay and casting wall favors heat conduction. In addition, the maximum temperature at different points with vibration is higher than that without vibration, demonstrating that the application of the mechanical vibration is favorable for raising the temperature of the filling front.

Temperature curves of four measuring points 1, 5, 9 and 13 in Fig. 3 close to the A356 inlay were selected to study the influence of the mechanical vibration on the temperature field in the vertical direction. The results are shown in Fig. 9. It can be seen that, no matter whether the vibration is applied or not, there is a large temperature difference between the different heights in the initial stage of the solidification, and the temperature between the different locations gradually tends to be consistent with the increase of the solidification time. However, by observing Regions I and II in Fig. 9, it can be found that, compared with the bimetallic samples without vibration, the temperature convergence rate at different points with vibration is significantly faster than that of the samples without vibration, indicating that the application of the mechanical vibration is conducive to the uniform distribution of the temperature field in the vertical direction. The highest temperatures of the temperature curves at different locations in Fig. 9 were counted and the results are shown in Table 3. The maximum temperature at different heights increases significantly after the application of the mechanical vibration. These results are consistent with the temperature profile in the horizontal direction. In addition, it can be found that, in the vertical direction, the closer to the top of the casting, the lower the maximum temperature, indicating that the temperature of the filling front is continuously decreasing.

To further analyze the influence of mechanical vibration on the solidification behavior of the Al/Mg bimetal, the temperature measurement points 9 and 10 were selected to calculate the temperature gradient in the horizontal direction, and the Points 9 and 13 were selected to calculate the temperature gradient in the vertical direction. The results are shown in Fig. 10.

It can be seen from Fig. 10(a) that there is a large horizontal temperature gradient in the initial solidification stage, which gradually decreases with increasing solidification time. In the initial solidification stage, the temperature gradient of the bimetal subjected to mechanical vibration is greater than that of the bimetal without vibration, but in the subsequent solidification process, the temperature gradient is smaller than that of the bimetal without mechanical vibration.

Table 2: Maximum temperatures in horizontal direction

Position	9	10	11	12
Without vibration	576.50 °C	600.89 °C	596.39 °C	589.60 °C
With vibration	587.13 °C	605.35 °C	616.65 °C	604.18 °C

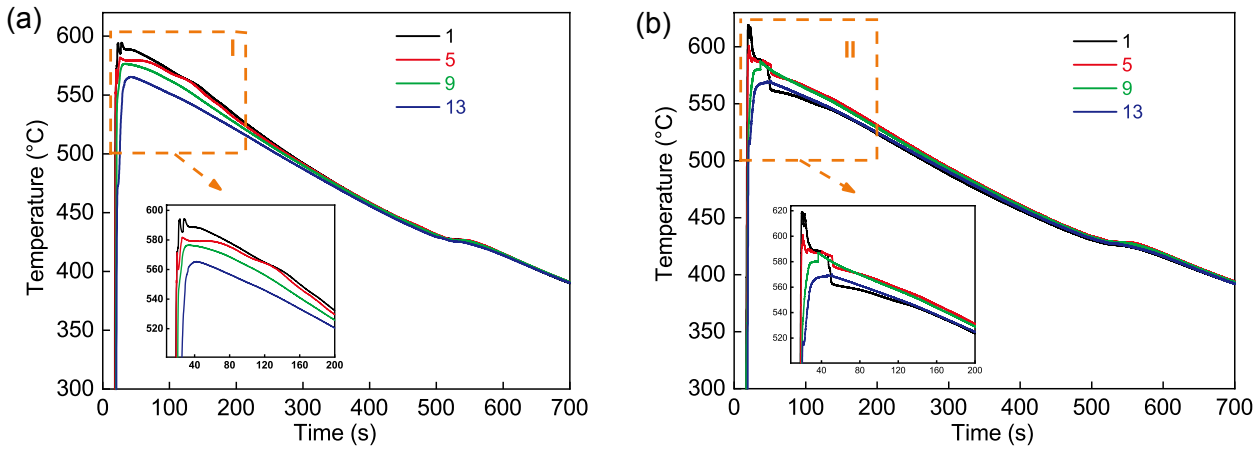

Fig. 9: Temperature curves in vertical direction without (a) and with (b) vibration

Table 3: Maximum temperatures in vertical direction

Position	1	5	9	13
Without vibration	594.40 °C	581.76 °C	576.50 °C	565.44 °C
With vibration	618.97 °C	600.98 °C	587.13 °C	570.11 °C

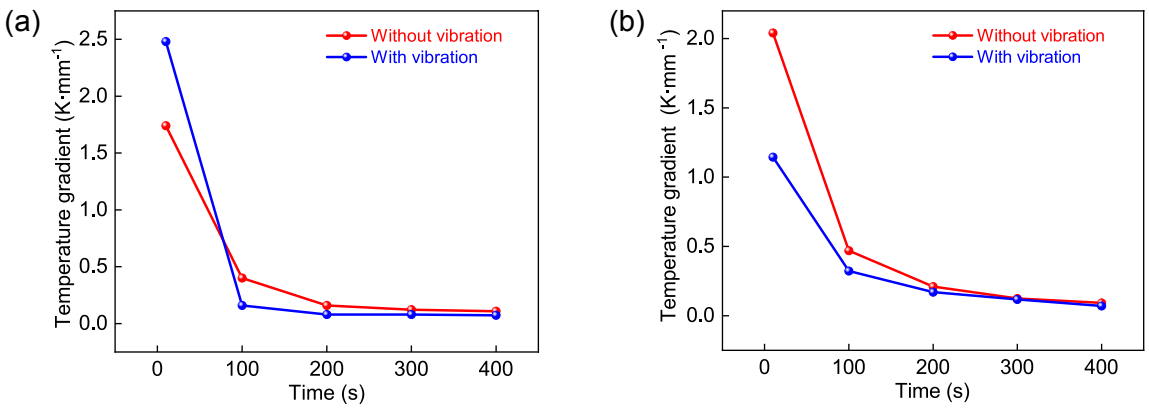

Fig. 10: Temperature gradients in horizontal (a) and vertical (b) direction

It can be seen from Fig. 10(b) that, at the initial solidification stage, there is a big temperature gradient in the vertical direction, but the temperature gradient gradually decreases with the solidification process. Moreover, the application of the mechanical vibration reduces the temperature gradient in the vertical direction compared to that without vibration. The above results further indicate that the mechanical vibration makes the temperature distribution in horizontal and vertical directions more uniform.

3.3 Microstructure and shear property

Figure 11 shows the microstructure images of the Al/Mg bimetal prepared without and with vibration (0.6 mm amplitude). It can be seen from the low-magnification images [Figs. 11(a) and (b)] that both AZ91D magnesium alloy and A356 aluminum alloy are connected by a metallurgical reaction layer. There are some inclusion defects in the metallurgical reaction layer of the Al/Mg bimetal without vibration, while no obvious inclusion defects are found in the Al/Mg bimetal with vibration. Through high-magnification images [Figs. 11(a1–a3) and (b1–b3)], it can be found that this interface layer is composed of Al_3Mg_2+Mg_2Si near A356 side, $Al_{12}Mg_{17}$+Mg eutectic structure near AZ91D side and $Al_{12}Mg_{17}$+Mg_2Si between them, which is consistent with our previous research [46]. The difference is that after the vibration is applied, the size of Mg_2Si particles and the number of the $Al_{12}Mg_{17}$ dendrites decrease, as shown in Figs. 11(a1–a3) and (b1–b3).

Figure 12 shows the shear strength of the bimetals before and after vibration (0.6 mm amplitude). It can be seen that the shear strength of the bimetal with vibration reaches 43.69 MPa, which is 39.76% higher than that without vibration (31.26 MPa). This indicates that the shear strength of the bimetal is significantly enhanced by the application of vibration.

4 Discussion

4.1 Influence mechanism of mechanical vibration on filling and solidification behavior

From the above results, it can be found that the filling and solidification processes of the solid-liquid composite Al/Mg bimetal by LFC are very different before and after the application of the mechanical vibration. This section is devoted to the effect mechanism of the mechanical vibrations on filling and solidification behavior, whose principle is illustrated in Fig. 13.

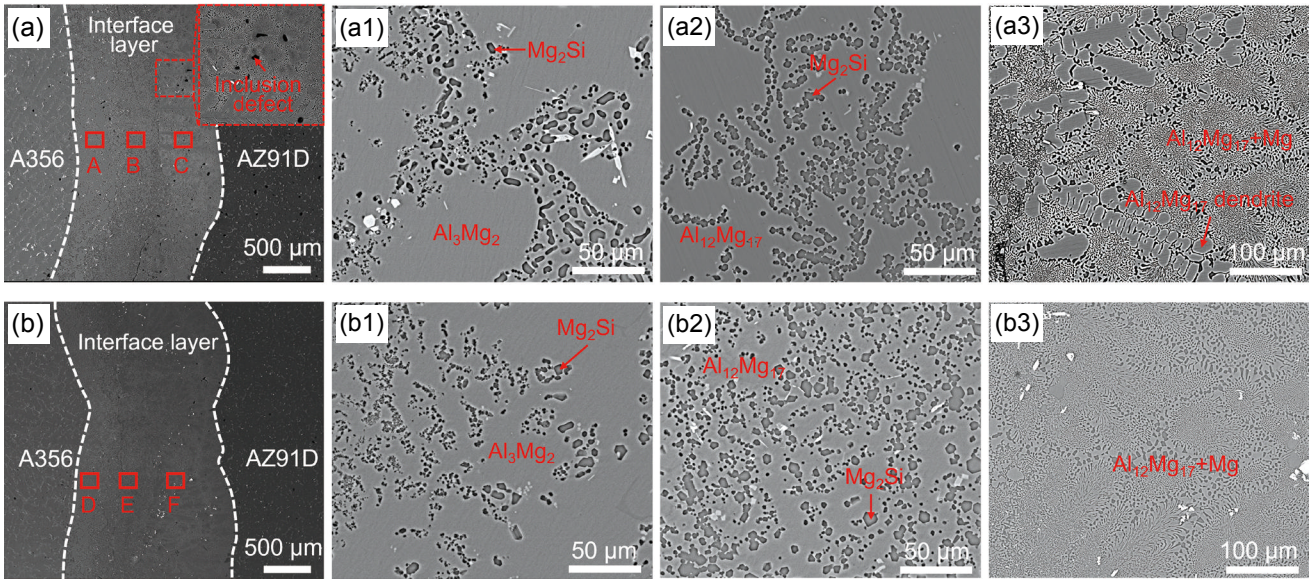

Fig. 11: Microstructures of Al/Mg bimetal: (a) without vibration; (a1), (a2), (a3) corresponding to Regions A, B, C, respectively; (b) with vibration; (b1), (b2), (b3) corresponding to Regions D, E, F, respectively

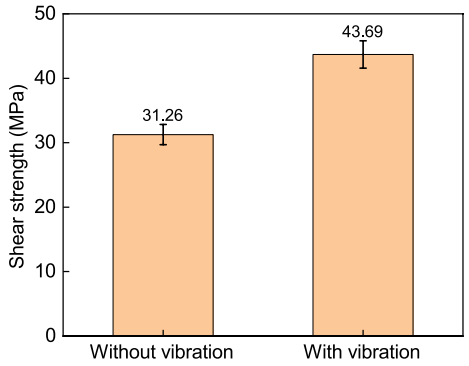

Fig. 12: Shear strengths of Al/Mg bimetals with and without vibration

When the hot metal liquid is poured into the mold cavity, the foam is decomposed into gaseous and liquid products due to the thermal action of the metal, and these products are expelled into the cavity through a breathable coating. There is a solid (cast wall)-liquid (AZ91D)-gas (gaseous decomposition products) three-phase interaction in the metal liquid front as same as traditional LFC [42]. However, this process also includes interactions among the liquid AZ91D, solid A356 and foam decomposition products due to the presence of the A356 inlay, which increases the complexity of metal-liquid pre-filling. As a result, this process is different from the filling process of the traditional LFC. Before and after the vibration is applied, the filling process of the metal liquid presents a concave shape, as

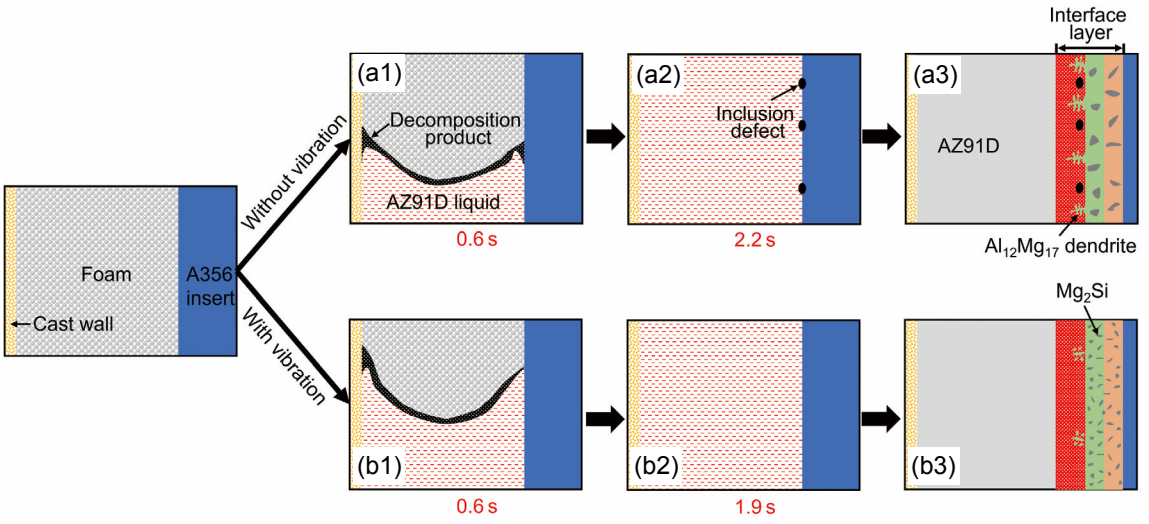

Fig. 13: Schematic diagram of influence mechanism of vibration on filling and solidification behavior

shown in Figs. 13(a1) and (b1). This is because the negative pressure is formed in the cavity under a vacuum, so that the filling velocity of the metal liquid near to the casting wall is greater than that of the metal liquid away from the casting wall, namely, the wall attachment effect. In addition, it can be found that there is a wall adhesion effect near the A356 inlay, which may be due to the gap between the A356 insert and the foam. The existence of the gap causes a negative pressure gradient from the A356 insert to the metal liquid, which reduces the filling resistance of the metal liquid front, therefore increasing the filling rate.

The wall attachment effect on the surface of the casting wall and the inlay exists regardless of whether the vibration is applied or not. However, the mechanical vibration has some different effects on the filling behavior of the solid-liquid composite Al/Mg bimetal by LFC, mainly as follows:

When no mechanical vibration is applied, there is a small air gap between the flow front of the metallic liquid and the A356 rod, while the contact is closer when the mechanical vibrations are applied. This is because, during the initial filling stage, the gap between the A356 inlay and the foam connects with the sandbox through breathable coating. Under the condition of vacuum-pumping, negative pressure will be formed in this area, which will accelerate the metal liquid filling and make the decomposition products of the EPS foam aggregate to the inlay surface. The metal liquid will wrap the decomposition products when they are too late to be discharged, which leads to the formation of the air gaps. The air gap would prevent a direct contact between the magnesium alloy liquid and the solid inlay. If these decomposition products are not completely expelled during the solidification process, the inclusion defects will be formed at the Al/Mg bimetallic interface, as displayed in Fig. 13(a2). After the mechanical vibration is applied, the heat exchange between the flow front of the metal liquid and the high temperature melt is facilitated, and the temperature of the filling front is increased. This will aggravate the thermal motion of the atoms in the liquid Mg on the flow front, reduce the surface tension of the Mg liquid, thus improving its wettability with the solid insert [9], as exhibited in Fig. 13(b2).

Mechanical vibration can improve the filling speed. The reasons are as follows: Firstly, the vibration can break and refine dendrite precipitates due to the temperature decrease of the magnesium alloy melt in the filling process, and the breaking of the dendrite can smooth the filling channel of the magnesium alloy liquid, thus increasing the filling rate [9]. Secondly, as the vibration amplitude is increased, the atomic motion in the

magnesium alloy liquid is intensified so that the interatomic binding force is reduced, which reduces the viscosity of the metallic liquid and the energy loss in the mould-filling process, thus the mould-filling capacity is increased. Thirdly, the thermal motion of the atoms and interatomic distance in the Mg melt increase under the action of the vibration, which decreases the surface tension of the Mg melt and is favorable for the Mg melt to flow forward. Thus, the fluidity of the magnesium alloy is enhanced, and the filling rate is accelerated. Fourthly, after applying mechanical vibrations, the heat exchange between the flow front of the metal liquid and the high temperature melt is facilitated, and the temperature of the filling front is increased, thus enhancing the fluidity of the magnesium alloy and accelerating the filling rate. However, when the amplitude exceeds a certain limit, the Al/Mg bimetallic filling rate decreases, which may be affected by the air gap pressure at the filling front. As the strength of the mechanical vibration increases, the heat exchange process between the flow front of the metal liquid and the high temperature melt is gradually enhanced, which causes the temperature of the filling front to gradually increase and accelerates the decomposition rate of the liquefied product of the foam. When the rate of foam decomposition is too fast to discharge, it obstructs the flow of liquid metal, therefore decreasing the filling rate.

Mechanical vibration makes the filling rate more balanced at different times. It can be found that the metal-liquid filling rate is fast at first and then slow no matter with or without vibration. The reason may be that as the filling process progresses, the temperature of the flow front of the Mg liquid gradually decreases, resulting in a weakening of the mobility and a reduction of the filling rate. After the mechanical vibration is applied, the temperature reduction of the metal-liquid front is slowed down because the heat exchange between the metal-liquid front and the high temperature melt is promoted, thus slowing down the decrease of liquidity and the filling rate.

The effect of mechanical vibration on solidification behavior of the Al/Mg bimetal prepared by LFC is mainly due to the reduction of the horizontal and vertical temperature gradients, which makes the temperature profile of the whole casting more uniform during the solidification process. This is because the vibration promotes heat transfer, and faster heat exchange makes the distribution of the temperature field more uniform throughout the casting.

4.2 Influence mechanism of mechanical vibration on microstructure and shear property

As can be seen from Section 3.3 that the mechanical vibration significantly improves the microstructure and shear properties of bimetals, and the affecting mechanisms are as follows:

Firstly, the mechanical vibration reduces the inclusion defects in the interface layer. As mentioned in Section 4.1, some decomposition products remain around the inlay because they cannot discharge out of the cavity in the filling process without vibration, which is the source of the inclusion defects, as shown in Fig. 13(a2). Under mechanical vibration, the temperature of the liquid front is higher, which favors the decomposition of the foam and floating of the decomposition products. In addition, the mechanical vibration also increases the wettability between the metallic liquid and the inlay, which also reduces the residual decomposition products in the interface region, thus reducing the inclusion defects, as indicated in Fig. 13(b2).

Secondly, the mechanical vibration reduces the size of the Mg_2Si particles in the interface layer and makes their distribution more uniform. According to our previous study, the Mg_2Si is formed by combining the Si in A356 and Mg diffused to the Al side [47]. When no vibration is applied, these Mg_2Si particles tend to form in situ due to the limited diffusion distance of the Si element, and the Mg_2Si with a relatively close distance is prone to agglomeration, so presenting the form of agglomeration distribution with large particles [47], as demonstrated in Fig. 13(a3). On the one hand, the vibration promotes the diffusion of elements, which increases the diffusion distance of the Si element. On the other hand, the vibration enhances the flow velocity and mutual shear between liquid and solid phase in the metallic liquid, which makes the Mg_2Si particles uniformly distribute in the interface layer with finer size, as exhibited in Fig. 13(b3).

Thirdly, the vibration reduces the $Al_{12}Mg_{17}$ dendrites. In the absence of the vibration, more $Al_{12}Mg_{17}$ dendrites are present in the interfacial layer. The generation of the $Al_{12}Mg_{17}$ dendrites in the Al/Mg bimetallic interface layer is caused by the inhomogeneous distribution of the element concentrations in the solidification front and the large condensate depression [47]. After the vibration is applied, the distribution of elements and temperature is more uniform, thus reducing the driving force for the generation of $Al_{12}Mg_{17}$ dendrites. In addition, the vibration increases the shear action of the solid and liquid during solidification, which may break up the $Al_{12}Mg_{17}$ dendrites that have already formed. As a result, the $Al_{12}Mg_{17}$ dendrites in the interface region are significantly reduced after vibration.

The shear properties of the bimetals are mainly determined by the interfacial microstructure characteristics. In general, the less the interfacial defects, the more homogeneous the microstructure distribution, and the smaller the grain size, the better the shear performance. Furthermore, the Mg_2Si has the effect of deflecting cracks and is the dominant strengthening phase in the bimetallic interface layer in the A356/AZ91D bimetals [38]. The smaller and more uniform the distribution of the Mg_2Si particles, the more it is resistant to cracking during deformation. Therefore, the improved bimetallic shear properties after vibration application can be attributed to the reduction of the interface defects, homogenization of the interface structure, and the generation of uniformly distributed small-sized Mg_2Si particles.

5 Conclusions

(1) The filling front of the solid-liquid composite Al/Mg bimetal in LFC presents a concave shape on both sides of the inlay, and the filling speed is firstly fast and then slow. Compared with the bimetal without vibration, the mechanical

vibration makes the filling more stable with a faster filling rate and increases the wettability between the liquid AZ91D and A356 inlays, thus eliminating the air gap between the A356 inlay and the AZ91D melt.

(2) Compared to the bimetal without vibration, the application of the mechanical vibration reduces the horizontal and vertical temperature gradient of the casting and increases the maximum temperature of the filling front. This is because the mechanical vibration can promote heat transfer, and faster heat exchange enhances the temperature of the filling front and the makes the temperature field distribution of the whole casting more uniform.

(3) The interface layer of the Al/Mg bimetal is composed of Al_3Mg_2+Mg_2Si near A356 side, $Al_{12}Mg_{17}$+Mg eutectic structure near AZ91D side and $Al_{12}Mg_{17}$+Mg_2Si between them whether the mechanical vibration is applied or not. The difference is the application of the vibration reduces the inclusion defects and $Al_{12}Mg_{17}$ dendrites and makes the Mg_2Si particles distribute evenly in a smaller size in the interface layer. Thus, the shear strength of the bimetal with vibration reaches 43.69 MPa, which is 39.76% higher than that without vibration (31.26 MPa).

Acknowledgements

This work was funded by the National Natural Science Foundation of China (Nos. 52075198, 52271102 and 52205359), the China Postdoctoral Science Foundation (No. 2021M691112). The authors also thank the support from the Analytical and Testing Center, HUST.

Conflict of interest

The authors declare that they have no conflict of interest.

References

[1] Zhu C, Zhao Z, Zhu Q, et al. Structures and macrosegregation of a 2024 aluminum alloy fabricated by direct chill casting with double cooling field. China Foundry, 2022, 19(1): 1–8.
[2] Su X, Huang J, Du X, et al. Influence of a low-frequency alternating magnetic field on hot tearing susceptibility of EV31 magnesium alloy. China Foundry, 2021, 18(3): 229–238.
[3] Yüksel Ç. Microstructural analysis of EN-GJS-450-10 ductile cast iron via vibrational casting. China Foundry, 2020, 17(4): 272–278.
[4] Chen X, Zhang Y, Lu Y, et al. Microstructure and mechanical properties of AZ91-Ca magnesium alloy cast by different processes. China Foundry, 2018, 15(4): 263–269.
[5] Luo A A, Sachdev A K, Apelian D. Alloy development and process innovations for light metals casting. Journal of Materials Processing Technology, 2022, 306: 117606.
[6] Baqer Y M, Ramesh S, Yusof F, et al. Challenges and advances in laser welding of dissimilar light alloys: Al/Mg, Al/Ti, and Mg/Ti alloys. The International Journal of Advanced Manufacturing Technology, 2018, 95(9): 4353–4369.
[7] Jadav H, Badheka V, Upadhyay G, et al. Dissimilar welding of magnesium alloy to aluminium alloy: A review. Advances in Materials and Processing Technologies, 2021: 1–28.
[8] Li G, Jiang W, Guan F, et al. Interfacial characteristics, mechanical properties and fracture behaviour of Al/Mg bimetallic composites by compound casting with different morphologies of Al insert. International Journal of Cast Metals Research, 2022, 35(4): 84–101.
[9] Wu C S, Wang T, Su H. Material flow velocity, strain and strain rate in ultrasonic vibration enhanced friction stir welding of dissimilar Al/Mg alloys. Journal of Manufacturing Processes, 2022, 75: 13–22.
[10] Zhao J, Wu C, Su H. Ultrasonic vibration-induced thinning of intermetallic compound layers in friction stir welding of dissimilar Al/Mg alloys. Science and Technology of Welding and Joining, 2022, 27(8): 621–628.
[11] Liu T, Song B, Huang G, et al. Preparation, structure and properties of Mg/Al laminated metal composites fabricated by roll-bonding, a review. Journal of Magnesium and Alloys, 2022, 10(8): 2062–2093.
[12] Zhang T, Wang Y, Xu Z, et al. A new method for fabricating Mg/Al alloy composites by pulse current-assisted rolled welding. Materials Letters, 2023, 330: 133247.
[13] Li G, Yang W, Jiang W, et al. The role of vacuum degree in the bonding of Al/Mg bimetal prepared by a compound casting process. Journal of Materials Processing Technology, 2019, 265: 112–121.
[14] Li G, Jiang W, Guan F, et al. Improving mechanical properties of AZ91D magnesium/A356 aluminum bimetal prepared by compound casting via a high velocity oxygen fuel sprayed Ni coating. Journal of Magnesium and Alloys, 2022, 10(4): 1075–1085.
[15] Li G, Jiang W, Guan F, et al. Design and achievement of metallurgical bonding of Mg/Al interface prepared by liquid-liquid compound casting via a co-deposited Cu-Ni alloy coating. Metallurgical and Materials Transactions A, 2022, 53(10): 3520.
[16] Zhang Z, Jiang W, Guan F, et al. Interface formation and strengthening mechanisms of Al/Mg bimetallic composite via compound casting with rare earth Ce introduction. Materials Science and Engineering: A, 2022, 854: 143830.
[17] Li G, Jiang W, Guan F, et al. Microstructure evolution, mechanical properties and fracture behavior of Al-*x*Si/AZ91D bimetallic composites prepared by a compound casting. Journal of Magnesium and Alloys, 2022, https://doi.org/10.1016/j.jma.2022.08.010.
[18] Song Q, Wang H, Ji S, et al. Improving joint quality of hybrid friction stir welded Al/Mg dissimilar alloys by RBFNN-GWO system. Journal of Manufacturing Processes, 2020, 59: 750–759.
[19] Hu W, Ma Z, Ji S, et al. Improving the mechanical property of dissimilar Al/Mg hybrid friction stir welding joint by PIO-ANN. Journal of Materials Science & Technology, 2020, 53: 41–52.
[20] Zhang H, Chen Y, Luo A A. A novel aluminum surface treatment for improved bonding in magnesium/aluminum bimetallic castings. Scripta Materialia, 2014, 86: 52–55.
[21] Zhang H, Chen Y, Luo A A. Improved interfacial bonding in magnesium/aluminum overcasting systems by aluminum surface treatments. Metallurgical and Materials Transactions B, 2014, 45(6): 2495–2503.
[22] Zhou J, Chen C, Zhou Z, et al. Dissimilar laser lap welding of Mg and Al alloys using a CoCrFeNi medium-entropy alloy interlayer. Optics & Laser Technology, 2023, 157: 108639.
[23] Yang H K, Qiu J, Cao C, et al. Theoretical design and experimental study of the interlayer of Al/Mg bimetallic composite plate by solid-liquid cast rolling. Materials Science and Engineering: A, 2022, 835: 142677.
[24] Li S, Zheng Z, Chang L, et al. A two-step bonding process for preparing 6061/AZ31 bimetal assisted with liquid molten zinc interlayer: The process and microstructure. Journal of Adhesion Science and Technology, 2022, 36(19): 2093–2115.

[25] Dong S, Lin S, Zhu H, et al. Effect of Ni interlayer on microstructure and mechanical properties of Al/Mg dissimilar friction stir welding joints. Science and Technology of Welding and Joining, 2022, 27(2): 103–113.
[26] Zhang Z, Jiang W, Li G, et al. Effect of La on microstructure, mechanical properties and fracture behavior of Al/Mg bimetallic interface manufactured by compound casting. Journal of Materials Science and Technology, 2022, 105: 214–225.
[27] Zhang Z, Jiang W, Li G, et al. Improved interface bonding of Al/Mg bimetal fabricated by compound casting with Nd addition. Materials Science and Engineering: A, 2021, 826: 141998.
[28] Arisova V N, Trykov Y P, Slautin O V, et al. Effect of heat treatment on mechanical properties and phase composition of magnesium-aluminum composite prepared by explosive welding. Metal Science and Heat Treatment, 2015, 57(5–6): 291–294.
[29] Yu Z, Wang T, Liu C, et al. Investigation on microstructure, mechanical properties and fracture mechanism of Mg/Al laminated composites. Materials Science and Engineering: A, 2022, 848: 143410.
[30] Zhu Z, Shi R, Klarner A D, et al. Predicting and controlling interfacial microstructure of magnesium/aluminum bimetallic structures for improved interfacial bonding. Journal of Magnesium and Alloys, 2020, 8(3): 578–586.
[31] Lyubimova T P, Parshakova Y N. Effect of rotational vibrations on directional solidification of high-temperature binary SiGe alloys. International Journal of Heat and Mass Transfer, 2018, 120: 714–723.
[32] Han Z, Wang Z, Sun Z, et al. Influence of non-uniform ultrasonic vibration on casting fluidity of liquid aluminum alloy. China Foundry, 2022, 19(5): 380–386.
[33] Fan S, Wu H, Fang J. Microstructure and mechanical properties of AZ91D magnesium alloy by expendable pattern shell casting with different mechanical vibration amplitudes and pouring temperatures. China Foundry, 2021, 18(1): 1–8.
[34] Zhao J, Wu C, Su H. Ultrasonic vibration-induced thinning of intermetallic compound layers in friction stir welding of dissimilar Al/Mg alloys. Science and Technology of Welding and Joining, 2022, 27(8): 621–628.
[35] He C, Wang T, Zhang Z, et al. Coupling effect of axial ultrasonic vibration and tool thread on the microstructure and properties of the friction stir lap welding joint of Al/Mg dissimilar alloys. Journal of Manufacturing Processes, 2022, 80: 95–107.
[36] Kumar S, Wu C. Suppression of intermetallic reaction layer by ultrasonic assistance during friction stir welding of Al and Mg based alloys. Journal of Alloys and Compounds, 2020, 827: 154343.
[37] Ji S, Meng X, Liu Z, et al. Dissimilar friction stir welding of 6061 aluminum alloy and AZ31 magnesium alloy assisted with ultrasonic. Materials Letters, 2017, 201: 173–176.
[38] Guan F, Fan S, Wang J, et al. Effect of vibration acceleration on interface microstructure and bonding strength of Mg-Al bimetal produced by compound casting. Metals, 2022, 12(5): 766.
[39] Wang J, Guan F, Jiang W, et al. The role of vibration time in interfacial microstructure and mechanical properties of Al/Mg bimetallic composites produced by a novel compound casting. Journal of Materials Research and Technology, 2021, 15: 3867–3879.
[40] Guan F, Jiang W, Wang J, et al. Development of high strength Mg/Al bimetal by a novel ultrasonic vibration aided compound casting process. Journal of Materials Processing Technology, 2022, 300: 117441.
[41] Huang J, Lin Y, Chen W, et al. Numerical analysis of lost foam casting for large-caliber water meter shell. Advances in Mechanical Engineering, 2021, 13(6): 16878140211028059.
[42] Ramesh R, Mohan S, Sivakumar N S, et al. Experimental investigation of lost foam casting process on aluminium. Materials Today: Proceedings, 2022, 50: 1134–1137.
[43] Paramasivam K, Anand M V, Sambathkumar M. Investigation of optimum process parameter of lost foam casting of A356/SiC metal matrix composite. Materials Today: Proceedings, 2021, 47: 4801–4806.
[44] Li G, Jiang W, Guan F, et al. Microstructure, mechanical properties and corrosion resistance of A356 aluminum/AZ91D magnesium bimetal prepared by a compound casting combined with a novel Ni-Cu composite interlayer. Journal of Materials Processing Technology, 2021, 288: 116874.
[45] Jezierski J, Jureczko M, Dojka R. The Impact of process factors on creating defects, mainly lustrous carbon, during the production of ductile iron using the lost-foam casting (LFC) method. Metals, 2020, 10(8): 1022.
[46] Fan S, Jiang W, Li G, et al. Fabrication and microstructure evolution of Al/Mg bimetal using a near-net forming process. Materials and Manufacturing Processes, 2017, 32(12): 1391–1397.
[47] Li G, Jiang W, Yang W, et al. New insights into the characterization and formation of the interface of A356/AZ91D bimetallic composites fabricated by compound casting. Metallurgical and Materials Transactions A, 2019, 50(2): 1076–1090.